Journal of
Mechanics of Materials and Structures

DISLOCATION INTERACTING WITH COLLINEAR RIGID LINES IN PIEZOELECTRIC MEDIA

BingJin Chen, DongWei Shu and ZhongMin Xiao

Volume 2, Nº 1 *January 2007*

mathematical sciences publishers

JOURNAL OF MECHANICS OF MATERIALS AND STRUCTURES
Vol. 2, No. 1, 2007

DISLOCATION INTERACTING WITH COLLINEAR RIGID LINES IN PIEZOELECTRIC MEDIA

BINGJIN CHEN, DONGWEI SHU AND ZHONGMIN XIAO

The electro-elastic interaction between a piezoelectric dislocation and collinear rigid lines embedded in a piezoelectric medium is studied in the framework of linear elastic theory. The rigid lines are considered, respectively, as dielectrics or conductors. We present a general solution of the problem based on the extended Stroh's formalism. Explicit expressions of the field intensity factors are obtained for the special case of a single rigid line. The image force acting on the piezoelectric dislocation due to the presence of a single rigid line is calculated by using the generalized Peach-Koehler formula. Numerical examples show the shielding effects of field intensity factors and image force on the dislocation. The solution we present can be served as a Green's function for investigating the micro-crack initiation mechanism at the tip of a rigid line.

1. Introduction

Piezoelectric materials are widely used in devices such as sensors and actuators. When subjected to mechanical and electric loads, these piezoelectric materials can fail prematurely due to defects arising in the manufacturing process. It is therefore important to study how defects such as dislocations and inclusions disturb the field variables, and how stress concentration arises as a result of defects. When a flat inclusion is much harder than the matrix, it is reasonable to consider it as a rigid line. There are numerous contributions to the literature on electro-elastic coupling characteristics of piezoelectric composite materials. To name a few, Pak [1992a] studied the anti-plane problem of a piezoelectric circular inclusion; Meguid and Zhong [1997] provided a general solution for the elliptical inhomogeneity problem in piezoelectric material under anti-plane shear and an in-plane electric field; Kattis et al. [1998] investigated the electro-elastic interaction effects of a piezoelectric screw dislocation with circular inclusion in piezoelectric material; Deng and Meguid [1998; 1999] considered the interaction between the piezoelectric elliptical inhomogeneity and a screw dislocation located inside inhomogeneity and outside inhomogeneity respectively under anti-plane shear and an in-plane electric field. More recently, Huang and Kuang [2001] evaluated the generalized electro-mechanical force for dislocation located inside, outside and on the interface of elliptical inhomogeneity in an infinite piezoelectric medium.

For rigid line problems in piezoelectric media, Liang et al. [1995] derived an exact general solution for an infinite piezoelectric medium with a rigid line and a crack. Shi [1997] investigated the collinear rigid lines under anti-plane deformation and in-plane electric field in piezoelectric media. Deng and Meguid [1998] addressed the plane problem of an interfacial rigid line between dissimilar piezoelectric materials. Gao and Fan [2000] investigated the generalized plane problem of piezoelectric media with collinear rigid lines under the loads at infinity. Chen et al. [2002] studied the problem of a screw dislocation

Keywords: rigid lines, dislocation, piezoelectric, field intensity factors, force on dislocation.

near a semi-infinite rigid line in a piezoelectric solid. More recently, Liu and Fang [2003] dealt with the interaction problem of a piezoelectric screw dislocation with circular interfacial rigid lines.

In the present work, we address the plane problem of a dislocation interacting with collinear rigid lines in piezoelectric media. Following this brief introduction, in Section 2 we outline the basic theory of the Stroh formalism. In Section 3 we state the problem to be investigated. We solve the problem of dielectric lines in Section 4 and that of conducting lines in Section 5. We present numerical examplesin Section 6, and concluding remarks in Section 7.

2. The Stroh formalism

In fixed rectangular coordinates x_i $(i = 1, 2, 3)$, the basic equations for linear piezoelectric materials at constant temperature can be written as

$$\sigma_{ij,j} = 0, \tag{2–1}$$

$$D_{i,i} = 0, \tag{2–2}$$

$$\gamma_{ij} = \tfrac{1}{2}(u_{i,j} + u_{j,i}), \tag{2–3}$$

$$E_i = -\phi_{,i}, \tag{2–4}$$

$$\sigma_{ij} = c_{ijkl}\gamma_{kl} - e_{kij}E_k, \tag{2–5}$$

$$D_i = e_{ikl}\gamma_{kl} + \varepsilon_{ik}E_k, \tag{2–6}$$

where σ_{ij}, γ_{ij}, u_i, D_i, E_i, ϕ are stress, strain, mechanical displacement, electric displacement, electric field and electric potential, respectively. c_{ijkl}, e_{kij} and ε_{ij} are the corresponding elastic, piezoelectric and dielectric constants, respectively, which satisfy the symmetric relations

$$c_{ijkl} = c_{klij} = c_{ijlk} = c_{jikl}, \qquad e_{kij} = e_{kji}, \qquad \varepsilon_{ik} = \varepsilon_{ki}, \tag{2–7}$$

where $i, j, k, l = 1, 2, 3$, repeated Latin indices mean summation, and a comma stands for partial differentiation.

Substitution of (2–3) and (2–4) into (2–5) and (2–6) yields

$$\sigma_{ij} = c_{ijkl}u_{k,l} + e_{kij}\phi_{,k}, \tag{2–8}$$

$$D_i = e_{ikl}u_{k,l} - \varepsilon_{ik}\phi_{,k}. \tag{2–9}$$

Furthermore, substituting (2–8) and (2–9) into (2–1) and (2–2) results in

$$(c_{ijkl}u_k + e_{lij}\phi)_{,li} = 0, \tag{2–10}$$

$$(e_{ikl}u_k - \varepsilon_{il}\phi)_{,li} = 0. \tag{2–11}$$

Here we only address a generalized two-dimensional deformation problem in the (x_1, x_2) plane. Therefore all the variables are constant along the x_3 axis. For such two-dimensional deformations where the physical quantities only depend on the coordinates x_1 and x_2, the general displacement solution to the above equations is

$$\boldsymbol{u} = \begin{Bmatrix} u_1 & u_2 & u_3 & u_4 \end{Bmatrix}^T = \boldsymbol{a} f(z), \quad z = x_1 + px_2, \tag{2–12}$$

or

$$u_k = a_k f(z), \quad k = 1, 2, 3, 4, \tag{2–13}$$

where $u_4 = \phi$ is the electric displacement, p and a are constants to be determined, and $f(z)$ is an arbitrary function of z. Substituting (2–12) into (2–10) and (2–11) yields

$$\big(c_{1jk1} + p(c_{2jk1} + c_{1jk2}) + p^2 c_{2jk2}\big)a_k + \big(e_{1j1} + p(e_{1j2} + e_{2j1}) + p^2 e_{2j2}\big)a_4 = 0, \tag{2–14}$$

$$\big(e_{1k1} + p(e_{1k2} + e_{2k1}) + p^2 e_{2k2}\big)a_k - \big(\varepsilon_{11} + p(\varepsilon_{12} + \varepsilon_{21}) + p^2 \varepsilon_{22}\big)a_4 = 0, \tag{2–15}$$

where $k = 1, 2, 3$. In view of (2–7), these equations can be rewritten as

$$\big(\boldsymbol{Q} + p(\boldsymbol{R} + \boldsymbol{R}^T) + p^2 \boldsymbol{T}\big)\boldsymbol{a} = 0, \tag{2–16}$$

where

$$Q_{ik} = c_{i1k1}, \qquad R_{ik} = c_{i1k2}, \qquad T_{ik} = c_{i2k2}. \tag{2–17}$$

The stresses and electric displacements can be expressed as

$$\sigma_{ij} = \big((c_{ijk1} + pc_{ijk2})a_k + (e_{1ji} + pe_{2ji})a_4\big)f'(z), \tag{2–18}$$

$$D_i = \big((e_{ik1} + pe_{ik2})a_k - (\varepsilon_{1i} + p\varepsilon_{2i})a_4\big)f'(z), \tag{2–19}$$

or

$$\{\sigma_{2j}, D_2\}^T = (\boldsymbol{R}^T + p\boldsymbol{T})\boldsymbol{a} f'(z), \qquad \{\sigma_{1j}, D_1\}^T = (\boldsymbol{Q} + p\boldsymbol{R})\boldsymbol{a} f'(z). \tag{2–20}$$

Defining

$$\boldsymbol{b} = (\boldsymbol{R}^T + p\boldsymbol{T})\boldsymbol{a}, \tag{2–21}$$

and comparing it with (2–16), we get

$$\boldsymbol{b} = (\boldsymbol{R}^T + p\boldsymbol{T})\boldsymbol{a} = -\frac{1}{p}(\boldsymbol{Q} + p\boldsymbol{R})\boldsymbol{a}. \tag{2–22}$$

By introducing the additional solution

$$\boldsymbol{\Phi} = \boldsymbol{b} f(z), \tag{2–23}$$

then (2–20) can be expressed as

$$\{\sigma_{2j}, D_2\}^T = \boldsymbol{\Phi}_{,1}, \qquad \{\sigma_{1j}, D_1\}^T = -\boldsymbol{\Phi}_{,2}. \tag{2–24}$$

The eigenvalue problem (2–16) gives four pairs of complex conjugates and corresponding vectors. p_α ($\alpha = 1, 2, 3, 4$) as the eigenvalues with positive imaginary part, and $\boldsymbol{a}_\alpha$ and $\boldsymbol{b}_\alpha$ as the associated vectors, we can write

$$p_{\alpha+4} = \bar{p}_\alpha, \qquad \boldsymbol{a}_{\alpha+4} = \bar{\boldsymbol{a}}_\alpha, \qquad \boldsymbol{b}_{\alpha+4} = \bar{\boldsymbol{b}}_\alpha, \tag{2–25}$$

where the over-bar denotes the complex conjugate. Assuming that p_α are distinct, the general solution can be written as

$$\boldsymbol{u} = \sum_{\alpha=1}^{4} \left(\boldsymbol{a}_\alpha f_\alpha(z_\alpha) + \bar{\boldsymbol{a}}_\alpha f_{\alpha+4}(\bar{z}_\alpha) \right), \tag{2–26}$$

$$\boldsymbol{\Phi} = \sum_{\alpha=1}^{4} \left(\boldsymbol{b}_\alpha f_\alpha(z_\alpha) + \bar{\boldsymbol{b}}_\alpha f_{\alpha+4}(\bar{z}_\alpha) \right), \tag{2–27}$$

where $z_\alpha = x_1 + p_\alpha x_2$ and f_l $(l = 1, 2, 3, 4, 5, 6, 7, 8)$ are arbitrary functions to be determined according to the boundary conditions. In many applications they could be assumed to have the same function form

$$f_\alpha(z_\alpha) = q_\alpha f(z_\alpha), \qquad f_{\alpha+4}(\bar{z}_\alpha) = \bar{q}_\alpha \bar{f}(\bar{z}_\alpha), \tag{2–28}$$

where q_α are constants to be determined, and $\bar{f}(\bar{z}_\alpha)$ is the conjugate complex of $f(z_\alpha)$. Defining two 4×4 complex matrices

$$\boldsymbol{A} = \begin{bmatrix} \boldsymbol{a}_1 & \boldsymbol{a}_2 & \boldsymbol{a}_3 & \boldsymbol{a}_4 \end{bmatrix}, \tag{2–29}$$

$$\boldsymbol{B} = \begin{bmatrix} \boldsymbol{b}_1 & \boldsymbol{b}_2 & \boldsymbol{b}_3 & \boldsymbol{b}_4 \end{bmatrix}, \tag{2–30}$$

Equations (2–26) and (2–27) can be written as

$$\boldsymbol{u} = \boldsymbol{A}\boldsymbol{f}(z) + \overline{\boldsymbol{A}\boldsymbol{f}}(\bar{z}), \tag{2–31}$$

$$\boldsymbol{\Phi} = \boldsymbol{B}\boldsymbol{f}(z) + \overline{\boldsymbol{B}\boldsymbol{f}}(\bar{z}), \tag{2–32}$$

where

$$\boldsymbol{f}(z) = \langle f(z_\alpha) \rangle \boldsymbol{q}, \tag{2–33}$$

with

$$\langle f(z_\alpha) \rangle = \operatorname{diag}\left[f(z_1), f(z_2), f(z_3), f(z_4) \right], \tag{2–34}$$

$$\boldsymbol{q} = \{q_1, q_2, q_3, q_4\}^T. \tag{2–35}$$

With the help of (2–22), the eigenvalue problem (2–16) can be expressed in a standard form as

$$\begin{bmatrix} -\boldsymbol{T}^{-1}\boldsymbol{R}^T & \boldsymbol{T}^{-1} \\ \boldsymbol{R}\boldsymbol{T}^{-1}\boldsymbol{R}^T - \boldsymbol{Q} & -\boldsymbol{R}\boldsymbol{T}^{-1} \end{bmatrix} \begin{bmatrix} \boldsymbol{a} \\ \boldsymbol{b} \end{bmatrix} = p \begin{bmatrix} \boldsymbol{a} \\ \boldsymbol{b} \end{bmatrix}, \tag{2–36}$$

The $\boldsymbol{A}$ and $\boldsymbol{B}$ expressed in (2–29) and (2–30) satisfy the normalized orthogonality relation

$$\begin{bmatrix} \boldsymbol{B}^T & \boldsymbol{A}^T \\ \bar{\boldsymbol{B}}^T & \bar{\boldsymbol{A}}^T \end{bmatrix} \begin{bmatrix} \boldsymbol{A} & \bar{\boldsymbol{A}} \\ \boldsymbol{B} & \bar{\boldsymbol{B}} \end{bmatrix} = \begin{bmatrix} \boldsymbol{I} & \boldsymbol{0} \\ \boldsymbol{0} & \boldsymbol{I} \end{bmatrix}, \tag{2–37}$$

from which three real 4×4 matrices can be defined

$$\boldsymbol{S} = i(2\boldsymbol{A}\boldsymbol{B}^T - \boldsymbol{I}), \qquad \boldsymbol{H} = 2i\boldsymbol{A}\boldsymbol{A}^T, \qquad \boldsymbol{L} = -2i\boldsymbol{B}\boldsymbol{B}^T, \tag{2–38}$$

where, $\boldsymbol{I}$ is the 4×4 identity matrix and $i=\sqrt{-1}$. It is easy to show that

$$\boldsymbol{HL}-\boldsymbol{SS}=\boldsymbol{LH}-\boldsymbol{S}^T\boldsymbol{S}^T=\boldsymbol{I},\qquad \boldsymbol{LS}+\boldsymbol{S}^T\boldsymbol{T}=\boldsymbol{SH}+\boldsymbol{HS}^T=\boldsymbol{0}. \tag{2–39}$$

For a dislocation $\boldsymbol{d}=[d_1,d_2,d_3,d_4]$ located at z_d in an infinite homogenous material, the vector $\boldsymbol{q}$ and the functions $f(z_\alpha)$ in (2–33) can be written as

$$\boldsymbol{q}=\frac{1}{2\pi i}\boldsymbol{B}^T\boldsymbol{d},\qquad f(z_\alpha)=\ln(z_\alpha-z_{d\alpha}). \tag{2–40}$$

Differentiating (2–31) and (2–32) with x_1, we obtain

$$\boldsymbol{u}_{,1}=\boldsymbol{AF}(z)+\overline{\boldsymbol{AF}}(\bar{z}), \tag{2–41}$$

$$\boldsymbol{\Phi}_{,1}=\boldsymbol{BF}(z)+\overline{\boldsymbol{BF}}(\bar{z})=i\boldsymbol{MAF}(z)-i\overline{\boldsymbol{MAF}}(\bar{z}), \tag{2–42}$$

where

$$\boldsymbol{F}(z)=d\boldsymbol{f}(z)/dz, \tag{2–43}$$

$$\boldsymbol{M}=-i\boldsymbol{BA}^{-1}=\boldsymbol{H}^{-1}+i\boldsymbol{H}^{-1}\boldsymbol{S}. \tag{2–44}$$

3. Statement of the problem

The physical problem to be investigated is shown in Figure 1. A charged dislocation $\boldsymbol{d}=[d_1,d_2,d_3,d_4]$ is located at the point $z_d(r_d,\theta_d)$ near some rigid lines L_r $(r=1,2,\ldots,N)$ embedded in an infinite piezoelectric medium. The rigid lines are assumed to be collinearly located along the x_1-axis of a Cartesian coordinate system $x_1x_2x_3$. The dislocation is assumed to be straight and infinitely long in the x_3-direction, suffering a finite discontinuity in the displacement and electric potential across the slip plane. Assume that the deformations of the solid depend on x_1 and x_2 only.

The mechanical boundary conditions at any rigid line surface are

$$u_j(t)^+=u_j(t)^-=u_{j0}+w_rx_1\delta_{j2},\quad j=1,2,3,\ t\in L_r, \tag{3–1}$$

where the superscript "+" and "−" refer, respectively, to the upper and lower rigid line surfaces, u_{j0} are displacements of the inclusions, w_r is the counterclockwise rotation with respect to the x_3 axis, and δ_{j2} is the Kronecker coefficient.

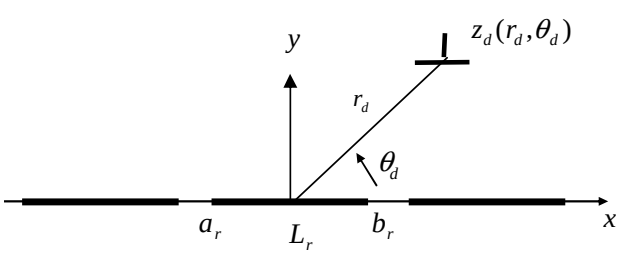

Figure 1. A piezoelectric screw dislocation near collinear rigid line inclusions.

The electric boundary conditions at any rigid line surface are

$$E_1(t)^+ = E_1(t)^-, \quad t \in L_r \tag{3–2a}$$

$$D_2(t)^+ = D_2(t)^-, \quad t \in L_r, \tag{3–2b}$$

for the dielectric rigid lines, and

$$u_4(t)^+ = u_4(t)^- = u_{40}, \quad t \in L_r \tag{3–3}$$

for the conducting rigid lines, where u_{40} is a constant.

By using the perturbation technique, the complex potential vectors for the current problem can be expressed as

$$\boldsymbol{F}(z) = \boldsymbol{F}_0(z) + \boldsymbol{F}_1(z), \tag{3–4}$$

where $\boldsymbol{F}_0(z)$ is associated with the unperturbed field that is related to the solutions of an infinite homogeneous medium without the inclusions and is holomorphic in the entire domain except at z_d. $\boldsymbol{F}_0(z)$ can be expressed as

$$\boldsymbol{F}_0(z) = \frac{1}{2\pi i}\left\langle \frac{1}{z_\alpha - z_{d\alpha}} \right\rangle \boldsymbol{B}^T \boldsymbol{d}. \tag{3–5}$$

The function $\boldsymbol{F}_1(z)$ corresponds to the perturbed field due to the introducing of the rigid lines and is holomorphic in the entire domain excluded the rigid lines. It is an unknown function to be determined according to the boundary conditions of the rigid lines.

4. Interaction of a dislocation with rigid dielectric lines

4.1. ***Determination of the complex potential function.*** In this case, the boundary conditions (3–1) and (3–2) apply. Conditions (3–1) and (3–2) can be rewritten as

$$u_j'(t)^+ = u_j'(t)^- = w_r \delta_{j2}, \qquad E_1(t)^+ = E_1(t)^-, \quad j = 1, 2, 3, \ t \in L_r, \tag{4–1}$$

$$D_2(t)^+ = D_2(t)^-, \quad t \in L_r, \tag{4–2}$$

where the prime denotes differentiation with respect to x_1. Using (2–41) and (3–4), condition (4–1) becomes

$$\boldsymbol{A}\boldsymbol{F}(t)^+ + \overline{\boldsymbol{A}\boldsymbol{F}}(t)^- = \boldsymbol{h}_0, \quad t \in L \tag{4–3}$$

$$\boldsymbol{A}\boldsymbol{F}(t)^- + \overline{\boldsymbol{A}\boldsymbol{F}}(t)^+ = \boldsymbol{h}_0, \quad t \in L \tag{4–4}$$

which leads to

$$[\boldsymbol{A}\boldsymbol{F}(t) - \overline{\boldsymbol{A}\boldsymbol{F}}(t)]^+ - [\ \boldsymbol{A}\boldsymbol{F}(t) - \overline{\boldsymbol{A}\boldsymbol{F}}(t)]^- = 0, \quad t \in L, \tag{4–5}$$

$$[\boldsymbol{A}\boldsymbol{F}(t) + \overline{\boldsymbol{A}\boldsymbol{F}}(t)]^+ + [\boldsymbol{A}\boldsymbol{F}(t) + \overline{\boldsymbol{A}\boldsymbol{F}}(t)]^- = 2\boldsymbol{h}_0, \quad t \in L, \tag{4–6}$$

where $\boldsymbol{h}_0(t) = (0, w_r, 0, -E_1(t))^T$, and $E_1(t)$ the unknown function that indicates the boundary value of

$E_1(z)$ on the inclusion faces [Gao and Fan 2000]. The substitution of (3–4) into (4–5) and (4–6) yields

$$[\boldsymbol{A}\boldsymbol{F}_1(t) - \overline{\boldsymbol{A}\boldsymbol{F}}_1(t)]^+ - [\boldsymbol{A}\boldsymbol{F}_1(t) - \overline{\boldsymbol{A}\boldsymbol{F}}_1(t)]^- = 0, \quad t \in L \tag{4–7}$$

$$[\boldsymbol{A}\boldsymbol{F}_1(t) + \overline{\boldsymbol{A}\boldsymbol{F}}_1(t)]^+ + [\boldsymbol{A}\boldsymbol{F}_1(t) + \overline{\boldsymbol{A}\boldsymbol{F}}_1(t)]^- = 2[\boldsymbol{h}_0(t) + \boldsymbol{h}(t)], \quad t \in L, \tag{4–8}$$

where

$$\boldsymbol{h}(t) = -\frac{\boldsymbol{A}}{2\pi i}\left\langle \frac{1}{t - z_{d\alpha}} \right\rangle \boldsymbol{B}^T \boldsymbol{d} + \frac{\bar{\boldsymbol{A}}}{2\pi i}\left\langle \frac{1}{t - \bar{z}_{d\alpha}} \right\rangle \bar{\boldsymbol{B}}^T \boldsymbol{d}. \tag{4–9}$$

Based on the theory of [Muskhelishvili 1975] and the assumption that $\boldsymbol{F}_1(z)$ vanishes at infinity, the solution of boundary problems (4–7) and (4–8) can be obtained as

$$\boldsymbol{A}\boldsymbol{F}_1(z) - \overline{\boldsymbol{A}\boldsymbol{F}}_1(z) = 0, \tag{4–10}$$

$$\boldsymbol{A}\boldsymbol{F}_1(z) + \overline{\boldsymbol{A}\boldsymbol{F}}_1(z) = \boldsymbol{h}_0(z) + 2[\boldsymbol{Z}(z) + X_0(z)\boldsymbol{P}(z)], \tag{4–11}$$

where

$$X_0(z) = \prod_{j=1}^{N} (z - a_j)^{-\frac{1}{2}} (z - b_j)^{-\frac{1}{2}}, \tag{4–12}$$

$$\boldsymbol{Z}(z) = \frac{X_0(z)}{2\pi i} \int_L \frac{\boldsymbol{h}(t)dt}{X_0^+(t)(t - z)}, \tag{4–13}$$

$$\boldsymbol{P}(z) = \boldsymbol{c}_N z^N + \boldsymbol{c}_{N-1} z^{N-1} + \cdots + \boldsymbol{c}_0. \tag{4–14}$$

Incorporating Equations (4–10) and (4–11) results in

$$\boldsymbol{A}\boldsymbol{F}_1(z) = \frac{\boldsymbol{h}_0(z)}{2} + \boldsymbol{Z}(z) + X_0(z)\boldsymbol{P}(z). \tag{4–15}$$

Taking the limit $z \to \infty$ in (4–15), and noting that $\boldsymbol{F}_1(\infty) = 0$, and $E_1(\infty) = 0$, the constant $\boldsymbol{c}_N$ can be obtained as

$$\boldsymbol{c}_N = (0, -w_r/2, 0, 0)^T. \tag{4–16}$$

The other constants, that is, the vector $\boldsymbol{c}_{N-1}, \ldots, \boldsymbol{c}_0$ and $w_N, \ldots, w_1$ can be determined by single-value displacement, the irrotationality of electric fields and the force equilibrium conditions. With reference to (2–42), these conditions can be written as

$$\oint_\Lambda \boldsymbol{A}\boldsymbol{F}_1(z)dz = 0, \qquad \hat{\boldsymbol{H}}_2 \oint_\Lambda \boldsymbol{A}\boldsymbol{F}_1(z)zdz = 0, \tag{4–17}$$

where Λ is the closed path around each inclusion, and $\hat{\boldsymbol{H}}_2$ is the second low of the real 4×4 matrix $\hat{\boldsymbol{H}} = \boldsymbol{H}^{-1}$. The complex potential is therefore obtained if the function $E_1(z)$ is known.

To obtain $E_1(z)$, we introduce the condition (4–2). Using (2–42), (4–2) can be rewritten as

$$i\boldsymbol{M}_4\boldsymbol{A}\boldsymbol{F}_1^+(t) - i\bar{\boldsymbol{M}}_4\overline{\boldsymbol{A}\boldsymbol{F}}_1^-(t) = i\boldsymbol{M}_4\boldsymbol{A}\boldsymbol{F}_1^-(t) - i\bar{\boldsymbol{M}}_4\overline{\boldsymbol{A}\boldsymbol{F}}_1^+(t), \tag{4–18}$$

where the vector $\boldsymbol{M}_4$ is the fourth low of the matrix $\boldsymbol{M}$ as expressed in (2–44). From [Muskhelishvili 1975] we know that the solution of the Equation (4–18) is

$$\hat{\boldsymbol{H}}_4\boldsymbol{A}\boldsymbol{F}_1(z) = 0, \tag{4–19}$$

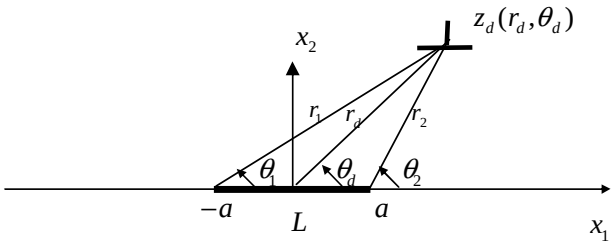

Figure 2. A piezoelectric screw dislocation near a rigid line inclusion.

where $\hat{\boldsymbol{H}}_4 = (\hat{H}_{41}, \hat{H}_{42}, \hat{H}_{43}, \hat{H}_{44})^T$ is the fourth low of the real 4×4 matrix $\hat{\boldsymbol{H}}$. Inserting (4–15) into (4–19) yields

$$E_1(z) = \frac{\hat{H}_{43}}{\hat{H}_{44}} w_r + \frac{2\hat{\boldsymbol{H}}_4}{\hat{H}_{44}}[\boldsymbol{Z}(z) + X_0(z)\boldsymbol{P}(z)]. \tag{4–20}$$

The complex potentials for the problem are thus determined. After $\boldsymbol{F}(z)$ has been obtained,we can calculate the stress and the electrical displacement fields. Thus, we can derive the field intensity factors and the force on the dislocation.

As an example, consider a single rigid line as shown in Figure 2. We can then simplify Equations (4–12) to (4–14) as

$$X_0(z) = (z^2 - a^2)^{-\frac{1}{2}}, \tag{4–21}$$

$$\boldsymbol{P}(z) = \boldsymbol{c}_1 z + \boldsymbol{c}_0, \tag{4–22}$$

$$\begin{aligned}\boldsymbol{Z}(z) = {} & \frac{\bar{\boldsymbol{A}}}{4\pi i}\left\langle \frac{1}{z_\alpha - \bar{z}_{d\alpha}} - \frac{\sqrt{\bar{z}_{d\alpha}{}^2 - a^2}}{\sqrt{z_\alpha{}^2 - a^2}(z_\alpha - \bar{z}_{d\alpha})} - \frac{1}{\sqrt{z_\alpha^2 - a^2}}\right\rangle \bar{\boldsymbol{B}}^T \boldsymbol{d} \\ & - \frac{\boldsymbol{A}}{4\pi i}\left\langle \frac{1}{z_\alpha - z_{d\alpha}} - \frac{\sqrt{z_{d\alpha}{}^2 - a^2}}{\sqrt{z_\alpha^2 - a^2}(z_\alpha - z_{d\alpha})} - \frac{1}{\sqrt{z_\alpha^2 - a^2}}\right\rangle \boldsymbol{B}^T \boldsymbol{d}.\end{aligned} \tag{4–23}$$

Substituting (4–15), together with (4–21), (4–22) and (4–23) into (4–17) yields

$$\boldsymbol{c}_0 = \boldsymbol{0}, \qquad \hat{\boldsymbol{H}}_2 \boldsymbol{c}_1 = 0. \tag{4–24}$$

Then, substituting (4–16) into (4–24) yields

$$\boldsymbol{c}_0 = \boldsymbol{0}, \qquad \boldsymbol{c}_1 = 0, \qquad w_r = 0, \tag{4–25}$$

The complex potentials are thus written as

$$\boldsymbol{A}\boldsymbol{F}_1(z) = (\boldsymbol{I} - \boldsymbol{Y})\boldsymbol{Z}(z), \tag{4–26}$$

where $\boldsymbol{I}$ is the 4×4 identity matrix, and

$$\boldsymbol{Y}=\begin{bmatrix} 0 & 0 & 0 & 0\\ 0 & 0 & 0 & 0\\ 0 & 0 & 0 & 0\\ \hat{H}_{41}/\hat{H}_{44} & \hat{H}_{42}/\hat{H}_{44} & \hat{H}_{43}/\hat{H}_{44} & 1 \end{bmatrix}. \tag{4–27}$$

When the material is purely elastic, the solution reduces to that of [Fan and Keer 1993].

4.2. ***Field intensity factors.*** Using (2–24), the field intensity factors at the right rigid line tip can be defined as

$$\boldsymbol{K}=\{K_{II},K_I,K_{II},K_D\}^T=\lim_{x_1\to a}\sqrt{2\pi(x_1-a)}\boldsymbol{\Phi}_{,1}(x_1), \tag{4–28}$$

where

$$\boldsymbol{\Phi}_{,1}(x_1)=2\,\mathrm{Re}\,i\boldsymbol{M}\boldsymbol{A}\boldsymbol{F}_1(x_1)=-2\boldsymbol{H}^{-1}\boldsymbol{S}(\boldsymbol{I}-\boldsymbol{Y})\,\mathrm{Re}\,\boldsymbol{Z}(x_1). \tag{4–29}$$

Substituting (4–23) into (4–29) yields

$$\boldsymbol{\Phi}_{,1}(x_1)=\frac{\boldsymbol{H}^{-1}\boldsymbol{S}(\boldsymbol{I}-\boldsymbol{Y})}{\pi\sqrt{x_1^2-a^2}}\left(\mathrm{Im}\,\boldsymbol{A}\left\langle\frac{\sqrt{x_1^2-a^2}-\sqrt{z_{d\alpha}^2-a^2}}{x_1-z_{d\alpha}}-1\right\rangle\boldsymbol{B}^T\boldsymbol{d}\right). \tag{4–30}$$

The field intensity factors are thus obtained as

$$\boldsymbol{K}=\frac{\boldsymbol{H}^{-1}\boldsymbol{S}(\boldsymbol{I}-\boldsymbol{Y})}{\sqrt{\pi a}}\left(\mathrm{Im}\,\boldsymbol{A}\left\langle\sqrt{\frac{z_{d\alpha}+a}{z_{d\alpha}-a}}-1\right\rangle\boldsymbol{B}^T\boldsymbol{d}\right). \tag{4–31}$$

When the dislocation lies along the real axis $z_d=(x_d,0)$, (4–15) reduces to

$$\boldsymbol{K}=-\frac{\boldsymbol{H}^{-1}\boldsymbol{S}(\boldsymbol{I}-\boldsymbol{Y})\boldsymbol{S}\boldsymbol{d}}{2\sqrt{\pi a}}\left(\sqrt{\frac{x_d+a}{x_d-a}}-1\right). \tag{4–32}$$

4.3. ***Force on dislocation.*** To analyze the possible balance position of a dislocation, it is of interest to compute the image force acting on the dislocation due to the presence of the rigid lines. The image force per unit length is defined as the negative gradient of the interaction energy with respect to the position of the dislocation. The image force [Pak 1990] can be written as

$$F_{x_1}=d_1\sigma_{21}^1+d_2\sigma_{22}^1+d_3\sigma_{23}^1+d_4D_2^1=\boldsymbol{d}^T\boldsymbol{\Phi}_{,1}^1, \tag{4–33}$$

$$F_{x_2}=-\left(d_1\sigma_{11}^1+d_2\sigma_{12}^1+d_3\sigma_{13}^1+d_4D_1^1\right)=\boldsymbol{d}^T\boldsymbol{\Phi}_{,2}^1, \tag{4–34}$$

where $\boldsymbol{\Phi}^1$ is associated with the perturbed field calculated from $\boldsymbol{F}_1(z)$ with $z_\alpha\to z_{d\alpha}$, that is,

$$\boldsymbol{F}_1(z_{d\alpha})=\frac{1}{2\pi i}\left[\boldsymbol{A}^{-1}(\boldsymbol{I}-\boldsymbol{Y})\bar{\boldsymbol{A}}\langle G_1\rangle\bar{\boldsymbol{B}}^T+\boldsymbol{A}^{-1}(\boldsymbol{I}-\boldsymbol{Y})\boldsymbol{A}\langle G_2\rangle\boldsymbol{B}^T\right]\boldsymbol{d}, \tag{4–35}$$

with

$$G_1(z_{d\alpha}) = \frac{\sqrt{z_{d\alpha}^2 - a^2} - \sqrt{\bar{z}_{d\alpha}^2 - a^2} - (z_{d\alpha} - \bar{z}_{d\alpha})}{2(z_{d\alpha} - \bar{z}_{d\alpha})\sqrt{z_{d\alpha}^2 - a^2}},$$
$$G_2(z_{d\alpha}) = -\frac{z_{d\alpha} - \sqrt{z_{d\alpha}^2 - a^2}}{2(z_{d\alpha}^2 - a^2)}. \tag{4–36}$$

As a result, we obtain

$$\boldsymbol{\Phi}_{,1}^1(z_{d\alpha}) = \frac{1}{\pi}\,\mathrm{Im}\left(\boldsymbol{B}\boldsymbol{A}^{-1}(\boldsymbol{I}-\boldsymbol{Y})\bar{\boldsymbol{A}}\langle G_1\rangle\bar{\boldsymbol{B}}^T + \boldsymbol{B}\boldsymbol{A}^{-1}(\boldsymbol{I}-\boldsymbol{Y})\boldsymbol{A}\langle G_2\rangle\boldsymbol{B}^T\right)\boldsymbol{d}, \tag{4–37}$$

$$\boldsymbol{\Phi}_{,2}^1(z_{d\alpha}) = \frac{1}{\pi}\,\mathrm{Im}\left(\boldsymbol{B}\boldsymbol{A}^{-1}(\boldsymbol{I}-\boldsymbol{Y})\bar{\boldsymbol{A}}\langle p_\alpha G_1\rangle\bar{\boldsymbol{B}}^T + \boldsymbol{B}\boldsymbol{A}^{-1}(\boldsymbol{I}-\boldsymbol{Y})\boldsymbol{A}\langle p_\alpha G_2\rangle\boldsymbol{B}^T\right)\boldsymbol{d}. \tag{4–38}$$

When the dislocation lies on the x_1-axis, that is, $z_{ad} = x_{1d} = x_d$, we can simplify the expressions (4–37) and (4–38)as

$$\boldsymbol{\Phi}_{,1}^1(x_d) = -g(x_d)\boldsymbol{H}^{-1}\boldsymbol{S}(\boldsymbol{I}-\boldsymbol{Y})\boldsymbol{S}\boldsymbol{d}, \tag{4–39}$$

$$\boldsymbol{\Phi}_{,2}^1(x_d) = g(x_d)\,\mathrm{Im}\left(\boldsymbol{B}\boldsymbol{A}^{-1}(\boldsymbol{I}-\boldsymbol{Y})\left(\bar{\boldsymbol{A}}\langle p_\alpha\rangle\bar{\boldsymbol{B}}^T - \boldsymbol{A}\langle p_\alpha\rangle\boldsymbol{B}^T\right)\right)\boldsymbol{d}, \tag{4–40}$$

where

$$g(x_d) = \frac{1}{2\pi}\frac{x_d - \sqrt{x_d^2 - a^2}}{x_d^2 - a^2}. \tag{4–41}$$

5. Interaction of a dislocation with rigid conducting lines

5.1. ***Determination of the complex potential function.*** In the case of rigid conducting lines, the boundary conditions (3–1) and (3–3) apply. Conditions (3–1) and (3–3) can be rewritten as

$$u_j'(t)^+ = u_j'(t)^- = w_r\delta_{j2}, \quad j = 1, 2, 3,\ t \in L_r \tag{5–1}$$

$$u_4'(t)^+ = u_4'(t)^- = 0, \quad t \in L_r, \tag{5–2}$$

where the prime denotes differentiation with respect to with x_1. With reference to (2–41) and (3–4), conditions (5–1) and (5–2) arrive at

$$\boldsymbol{A}\boldsymbol{F}(t)^+ + \overline{\boldsymbol{A}\boldsymbol{F}}(t)^- = \boldsymbol{h}_0, \quad t \in L, \tag{5–3}$$

$$\boldsymbol{A}\boldsymbol{F}(t)^- + \overline{\boldsymbol{A}\boldsymbol{F}}(t)^+ = \boldsymbol{h}_0, \quad t \in L, \tag{5–4}$$

which lead to

$$\left[\boldsymbol{A}\boldsymbol{F}(t) - \overline{\boldsymbol{A}\boldsymbol{F}}(t)\right]^+ - \left[\boldsymbol{A}\boldsymbol{F}(t) - \overline{\boldsymbol{A}\boldsymbol{F}}(t)\right]^- = 0, \quad t \in L, \tag{5–5}$$

$$\left[\boldsymbol{A}\boldsymbol{F}(t) + \overline{\boldsymbol{A}\boldsymbol{F}}(t)\right]^+ + \left[\boldsymbol{A}\boldsymbol{F}(t) + \overline{\boldsymbol{A}\boldsymbol{F}}(t)\right]^- = 2\boldsymbol{h}_0, \quad t \in L, \tag{5–6}$$

where $\boldsymbol{h}_0 = (0, w_r, 0, 0)^T$. Substituting (3–4) into (5–5) and (5–6) yields

$$\left[\boldsymbol{A}\boldsymbol{F}_1(t) - \overline{\boldsymbol{A}\boldsymbol{F}}_1(t)\right]^+ - \left[\boldsymbol{A}\boldsymbol{F}_1(t) - \overline{\boldsymbol{A}\boldsymbol{F}}_1(t)\right]^- = 0, \quad t \in L, \tag{5–7}$$

$$\left[\boldsymbol{A}\boldsymbol{F}_1(t) + \overline{\boldsymbol{A}\boldsymbol{F}}_1(t)\right]^+ + \left[\boldsymbol{A}\boldsymbol{F}_1(t) + \overline{\boldsymbol{A}\boldsymbol{F}}_1(t)\right]^- = 2[\boldsymbol{h}_0 + \boldsymbol{h}(t)], \quad t \in L, \tag{5–8}$$

where $\boldsymbol{h}(t)$ is as defined in (4–9). This problem is a special case of the case solved in the previous section. The solution can be obtained from the previous solution by setting $\boldsymbol{Y} = \boldsymbol{0}$. For a single rigid conducting line as shown in Figure 2, the complex potential corresponding to the perturbed field is

$$\boldsymbol{A}\boldsymbol{F}_1(z) = \boldsymbol{Z}(z), \tag{5–9}$$

where $\boldsymbol{Z}(z)$ is as in (4–23).

5.2. ***Field intensity factors.*** The field intensity factors at the right inclusion tip can be defined as

$$\boldsymbol{K} = \frac{\boldsymbol{H}^{-1}\boldsymbol{S}}{\sqrt{\pi a}}\left(\operatorname{Im} A\left\langle\sqrt{\frac{z_{d\alpha}+a}{z_{d\alpha}-a}} - 1\right\rangle \boldsymbol{B}^T\boldsymbol{d}\right). \tag{5–10}$$

When the dislocation lies along the real axis $z_d = (x_d, 0)$, Equation (5–15) reduces to

$$\boldsymbol{K} = -\frac{\boldsymbol{H}^{-1}\boldsymbol{S}^2\boldsymbol{d}}{2\sqrt{\pi a}}\left(\sqrt{\frac{x_d+a}{x_d-a}} - 1\right). \tag{5–11}$$

5.3. ***Force on dislocation.*** The image force on dislocation can be written as

$$F_{x_1} = \boldsymbol{d}^T\boldsymbol{\Phi}^1_{,1}(z_{d\alpha}), \tag{5–12}$$

$$F_{x_2} = \boldsymbol{d}^T\boldsymbol{\Phi}^1_{,2}(z_{d\alpha}), \tag{5–13}$$

where

$$\boldsymbol{\Phi}^1_{,1}(z_{d\alpha}) = \frac{1}{\pi}\operatorname{Im}\left[\boldsymbol{B}\boldsymbol{A}^{-1}\bar{\boldsymbol{A}}\langle G_1\rangle\bar{\boldsymbol{B}}^T + \boldsymbol{B}\langle G_2\rangle\boldsymbol{B}^T\right]\boldsymbol{d}, \tag{5–14}$$

$$\boldsymbol{\Phi}^1_{,2}(z_{d\alpha}) = \frac{1}{\pi}\operatorname{Im}\left[\boldsymbol{B}\boldsymbol{A}^{-1}\bar{\boldsymbol{A}}\langle p_\alpha G_1\rangle\bar{\boldsymbol{B}}^T + \boldsymbol{B}\langle p_\alpha G_2\rangle\boldsymbol{B}^T\right]\boldsymbol{d}. \tag{5–15}$$

$G_1(z_{d\alpha})$ and $G_2(z_{d\alpha})$ are as defined in (4–36). When the dislocation lies on the x_1-axis, that is, $z_{da} = x_{1d} = x_d$, we simplify (5–14) and (5–15) as

$$\boldsymbol{\Phi}^1_{,1}(x_d) = g(x_d)(\boldsymbol{H}^{-1} - \boldsymbol{L})\boldsymbol{d}, \tag{5–16}$$

$$\boldsymbol{\Phi}^1_{,2}(x_d) = g(x_d)\operatorname{Im}\left\{\boldsymbol{B}\boldsymbol{A}^{-1}[\bar{\boldsymbol{A}}\langle p_\alpha\rangle\bar{\boldsymbol{B}}^T - \boldsymbol{A}\langle p_\alpha\rangle\boldsymbol{B}^T]\right\}\boldsymbol{d}, \tag{5–17}$$

where $g(x_d)$ is as defined in (4–41).

6. Numerical examples

The previous sections derived the explicit expressions for the field intensity factors and the forces on the dislocation. However they are not straightforward since several variables are involved. In this section, we present some numerical illustrations. As an example, we address the case when the dislocation lies

along $\theta_d = \pi/6$. The material is assumed to be PZT-5H, with the x_1-axis the polling direction. The material constants [Pak 1992b] are

$$\begin{aligned}
&c_{11} = 117\,\text{GPa}, \qquad c_{12} = c_{13} = 53\,\text{GPa},\\
&c_{22} = c_{33} = 126\,\text{GPa}, \qquad c_{23} = 55\,\text{GPa},\\
&c_{44} = 35.5\,\text{GPa}, \qquad c_{55} = c_{66} = 35.3\,\text{GPa},\\
&e_{11} = 23.3\,\text{C/m}^2, \qquad e_{12} = e_{13} = -6.5\,\text{C/m}^2,\\
&e_{35} = e_{26} = 17\,\text{C/m}^2,\\
&\varepsilon_{11} = 130 \times 10^{-10}\,\text{C/Vm},\\
&\varepsilon_{22} = \varepsilon_{33} = 151 \times 10^{-10}\,\text{C/Vm}.
\end{aligned} \tag{6–1}$$

For p_α $(\alpha = 1, 2, 3, 4)$, the values of $\boldsymbol{A}$ and $\boldsymbol{B}$ are then calculated as follows:

$$\begin{aligned}
p_1 &= -0.17351 + 0.93175i,\\
p_2 &= 0.17351 + 0.93175i,\\
p_3 &= 0.93367i,\\
p_4 &= 0.99718i,
\end{aligned} \tag{6–2}$$

$$\begin{aligned}
&A_{11} = -.8521 \times 10^{-6} + .3117 \times 10^{-5}i, \qquad A_{12} = .3117 \times 10^{-5} - .8521 \times 10^{-6}i,\\
&A_{13} = .4133 \times 10^{-5} + .1433 \times 10^{-5}i, \qquad A_{14} = 0,\\
&A_{21} = -.3561 \times 10^{-5} + .4268 \times 10^{-6}i, \qquad A_{22} = -.4268 \times 10^{-6} + .3561 \times 10^{-5}i,\\
&A_{23} = -.1189 \times 10^{-5} + .1189 \times 10^{-5}i, \qquad A_{24} = 0,\\
&A_{31} = 0, \qquad A_{32} = 0,\\
&A_{33} = 0, \qquad A_{34} = -.2657 \times 10^{-5} + .2657 \times 10^{-5}i,\\
&A_{41} = 722.3288 + 2351.6593i, \qquad A_{42} = 2351.6593 + 722.3288i,\\
&A_{43} = -3006.4445 - 3006.4445i, \qquad A_{44} = 0.
\end{aligned} \tag{6–3}$$

$$\begin{aligned}
&B_{11} = -262382.5644 - 27548.9152i, \qquad B_{12} = 27548.9157 + 262382.5653i,\\
&B_{13} = -41491.1280 + 41491.1353i, \qquad B_{14} = 0,\\
&B_{21} = -22107.3141 - 277484.1268i, \qquad B_{22} = -277484.1276 - 22107.3141i,\\
&B_{23} = 44438.6631 - 44438.6550i, \qquad B_{24} = 0,\\
&B_{31} = 0, \qquad B_{32} = 0, \qquad B_{33} = 0, \qquad B_{34} = -94074.2510 - 94074.2510i,\\
&B_{41} = -.7241 \times 10^{-4} - .1944 \times 10^{-4}i, \qquad B_{42} = .1944 \times 10^{-4} + .7241 \times 10^{-4}i,\\
&B_{43} = -.8535 \times 10^{-4} + .8535 \times 10^{-4}i, \qquad B_{44} = 0.
\end{aligned} \tag{6–4}$$

6.1. ***Field intensity factors.*** The expression (4–31) gives the field intensity factors at the right rigid line tip arising from the dislocation $\boldsymbol{d} = (d_1, d_2, d_3, d_4)^T$ located at z_d near a rigid dielectric line. Expression (5–10) does the same for a rigid conducting line. When these intensity factors have the same sign as

those arising from the remote applied stress or electric displacement, the total intensity factors increase. The dislocation then anti-shields the rigid line tip; otherwise the dislocation shields it. Shielding effects from d_1, d_2, and d_4 on K_I, K_{II}, K_{III}, K_D for the dislocation located along $\theta_d = \pi/6$ near a rigid line are illustrated in Figures 3 to 8, in relation to the normalized dislocation radial location r_d/a. To plot the four field intensity factors in one figure, the values of K_I, K_{II}, K_{III}, K_D were properly normalized in the figures with positive values. The normalized intensity factors are denoted as K_I^*, K_{II}^*, K_{III}^*, K_D^* in the figures, where

$$K_j^*(d_j) = \frac{K_j(d_j)}{K_{j0}(d_j)}, \quad j = I, II, III, D, \tag{6–5}$$

with

$$\begin{aligned} &K_{j0}(d_j) = \frac{d_j}{2\sqrt{\pi a}} \times 10^{10}\,\mathrm{N/m^2}, \qquad K_{D0}(d_j) = \frac{d_j}{\sqrt{\pi a}} \times 2\,\mathrm{N/Vm}, \quad j = I, II, III \\ &K_{j0}(d_4) = \frac{d_4}{\sqrt{\pi a}} \times 2\,\mathrm{N/Vm}, \quad j = I, II, III, \qquad K_{D0}(d_4) = \frac{d_4}{\sqrt{\pi a}} \times 10^{-9}\,\mathrm{N/V^2}. \end{aligned} \tag{6–6}$$

In the above equations, $d_I = d_1$, $d_{II} = d_2$, $d_{III} = d_3$.

Figure 3 shows that the glide dislocation d_1 always shields K_I while anti-shielding K_{II} and K_D when it is near a dielectric line tip. The shielding effects from the glide dislocation on K_{II} and K_D appear

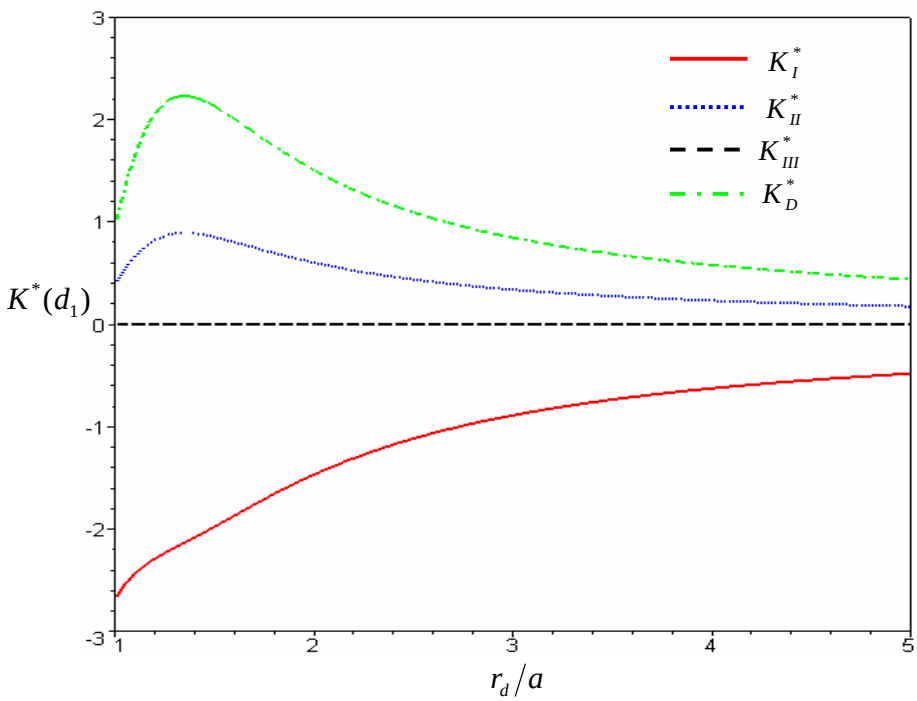

Figure 3. The shielding effect from the glide dislocation d_1 located along $\theta_d = \pi/6$ on the field intensity factors for a rigid dielectric inclusion.

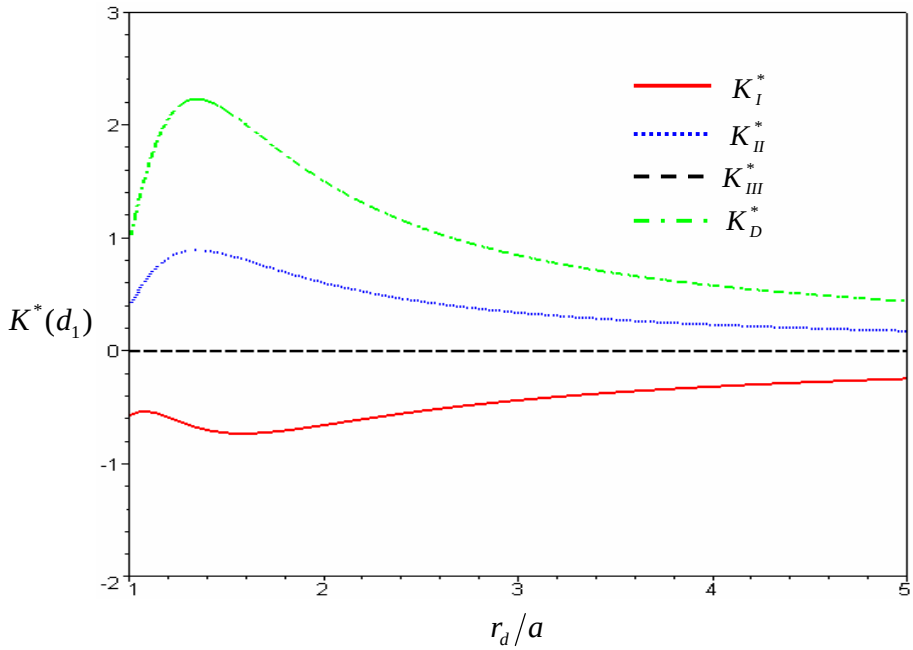

Figure 4. The shielding effect from the glide dislocation d_1 located along $\theta_d = \pi/6$ on the field intensity factors for a rigid conducting inclusion.

in a very similar way. But the glide dislocation d_1 does not affect K_{III}. This occurs because the glide dislocation does not contribute any anti-plane deformations.

Figure 4 also shows that the glide dislocation d_1 always shields K_I while anti-shielding K_{II} and K_D, but does not affect K_{III} when it is near a conducting line tip. A comparison of Figures 3 and 4 indicates that the conductivity of the inclusion only has apparent effects on K_I.

Figures 5 and 6 show the shielding effects from the climb dislocation d_2 for a rigid dielectric line and a rigid conducting line, respectively. We find that the two figures are nearly the same, which indicates that the conductivity of the rigid line is not sensitive to the shielding effects from d_2.

Figures 7 and 8 show the shielding effects from the electrical dislocation d_4 for a rigid dielectric line and a rigid conducting one, respectively. The comparison of these two figures also indicates that the conductivity of the rigid line only has apparent effects on K_I. For a rigid dielectric line, it first anti-shields and then shields K_I when increasing r_d/a; while for a rigid conducting one, it always shields K_I.

6.2. ***Image force on dislocation.*** Expressions for the image forces on the dislocation due to existence of the inclusion are calculated using (4–33) and (4–34) together with (4–37) and (4–38) for a rigid dielectric line, and by (5–12) to (5–15) for a rigid conducting one. As such, the slip and climb parts of the image forces can be calculated as follows:

$$\begin{aligned} F_r &= F_x \cos\theta_d + F_y \sin\theta_d, \\ F_t &= -F_x \sin\theta_d + F_y \cos\theta_d. \end{aligned} \tag{6–7}$$

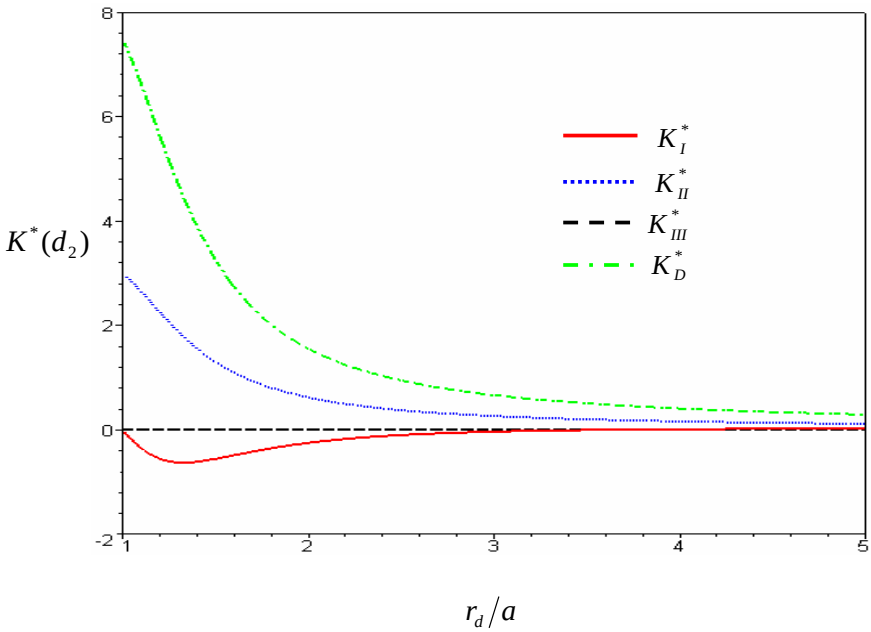

Figure 5. The shielding effect from the climb dislocation d_2 located along $\theta_d = \pi/6$ on the field intensity factors for a rigid dielectric inclusion.

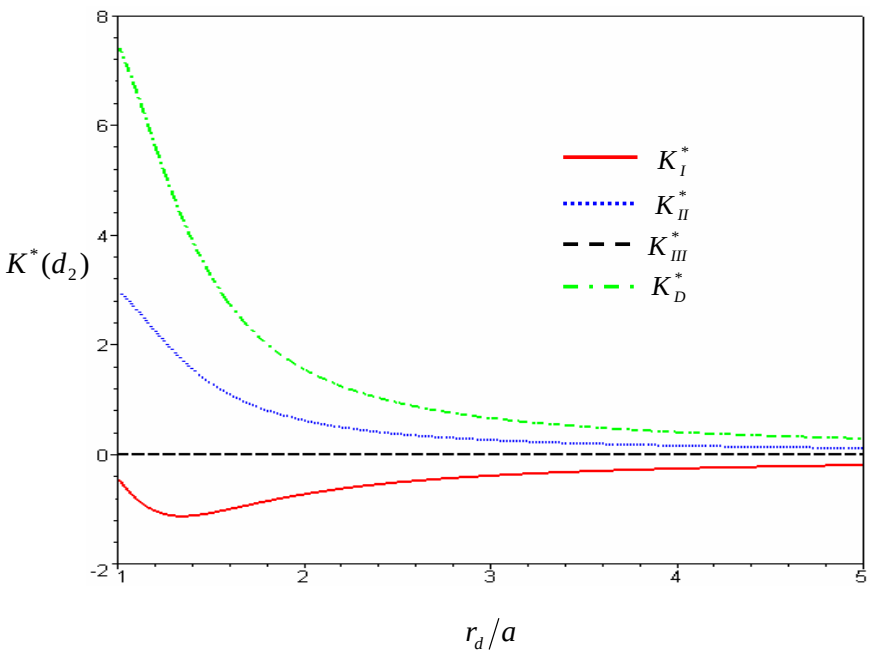

Figure 6. The shielding effect from the climb dislocation d_2 located along $\theta_d = \pi/6$ on the field intensity factors for a rigid conducting inclusion.

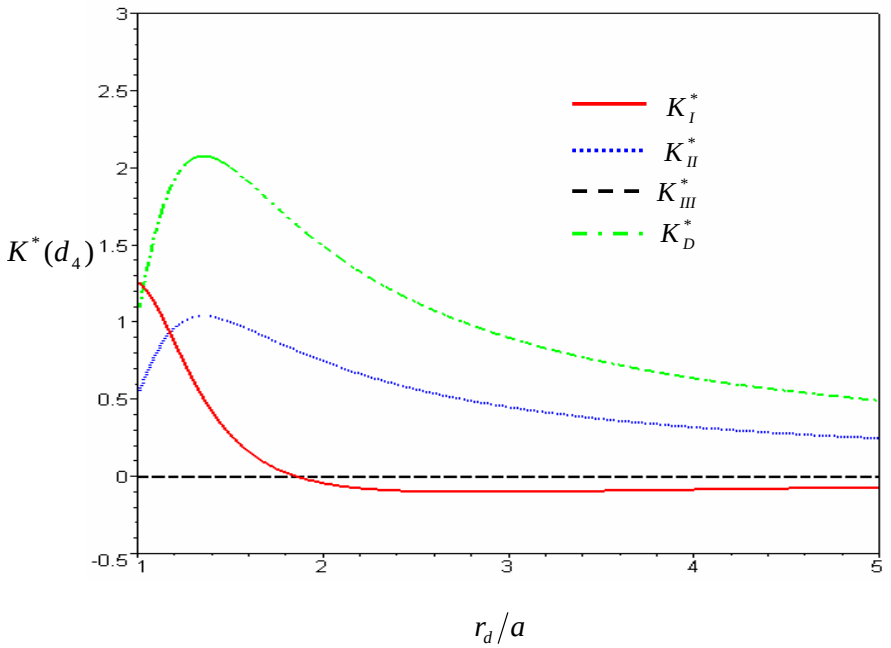

Figure 7. The shielding effect from the electrical dislocation d_4 located along $\theta_d = \pi/6$ on the field intensity factors for a rigid dielectric inclusion.

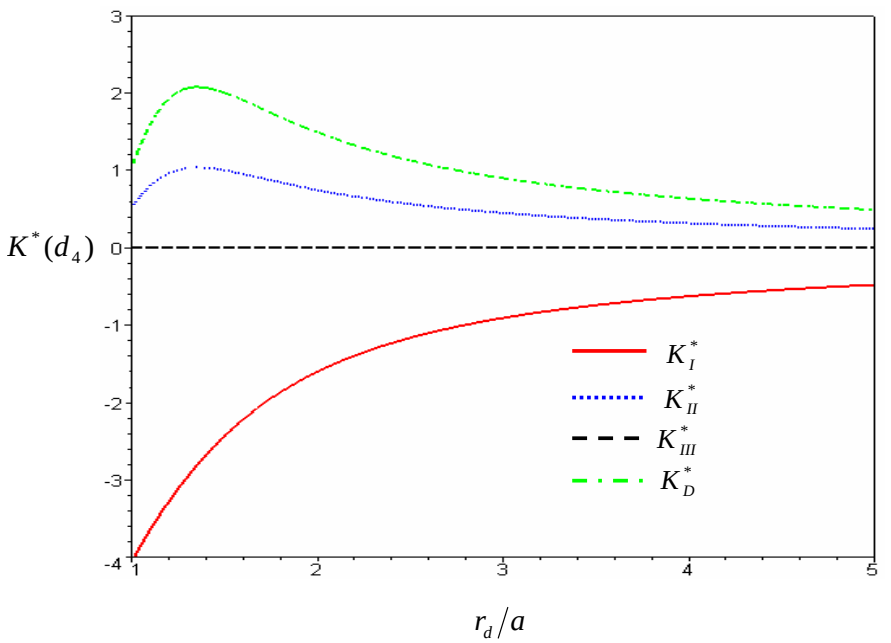

Figure 8. The shielding effect from the electrical dislocation d_4 located along $\theta_d = \pi/6$ on the field intensity factors for a rigid conducting inclusion.

Figures 9 and 10 plot the normalized slip image force F_r/F_0 and climb image force F_t/F_0 varied with the normalized radial location r_d/a, respectively, for a rigid *dielectric* line.

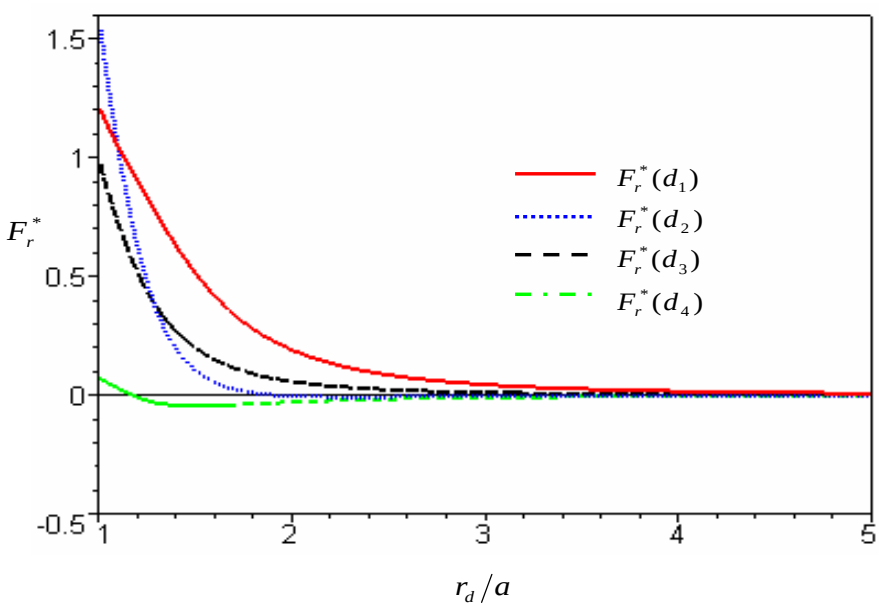

Figure 9. Variations of the radial normalized image forces on the dislocation located along $\theta_d = \pi/6$ near a rigid dielectric inclusion.

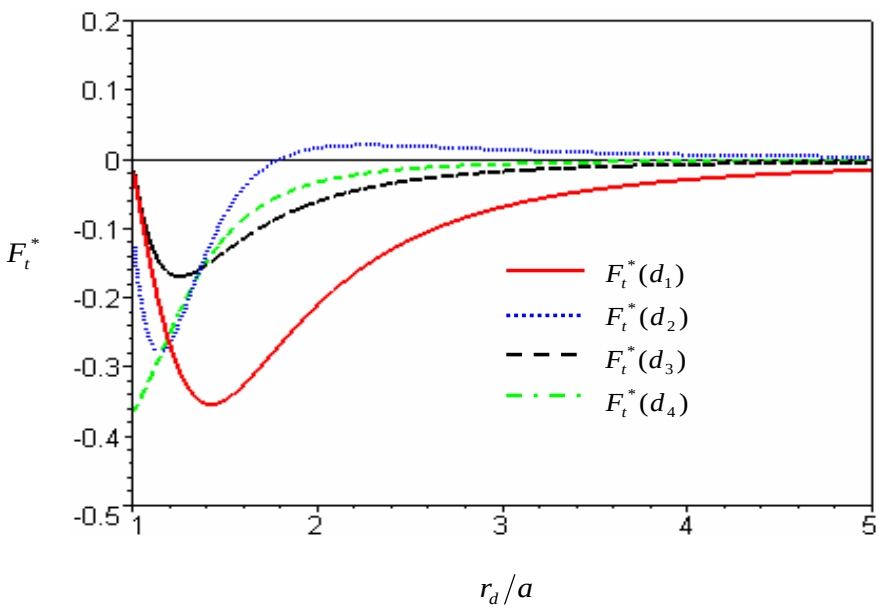

Figure 10. Variations of the tangential normalized image forces on the dislocation located along $\theta_d = \pi/6$ near a rigid dielectric inclusion.

Figures 11 and 12 plot those for a rigid *conducting* line. The dislocation has four different dislocation strength characteristics (d_1, d_2, d_3, d_4). We allow the dislocation to have only one non-zero strength

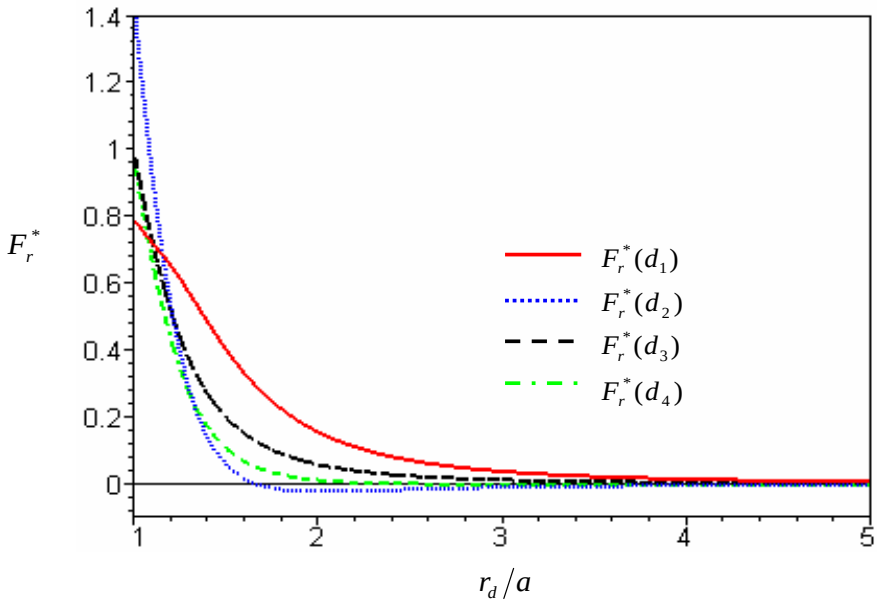

Figure 11. Variations of the radial normalized image forces on the dislocation located along $\theta_d = \pi/6$ near a rigid conducting inclusion.

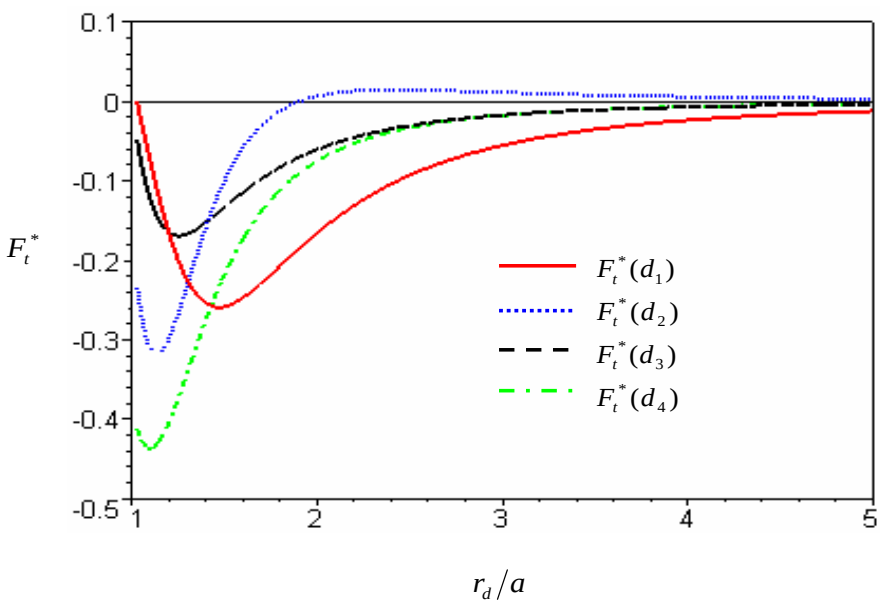

Figure 12. Variations of the tangential normalized image forces on the dislocation located along $\theta_d = \pi/6$ near a rigid conducting inclusion.

characteristic. The other three are zero in each plotted curve. The normalizing factors in each curve are given by

$$F_0 = \frac{\boldsymbol{d}^T \boldsymbol{L}\boldsymbol{d}}{4\pi a}. \tag{6–8}$$

Figures 9 and 10 show that, a rigid dielectric line always repels the mechanical dislocation in the radial direction, while it does little on the electrical dislocation; it always attracts the dislocation to the real axis when it is close to the rigid line tip. On the other hand, Figures 11 and 12 show that a rigid conducting line always repels the dislocation in the radial direction and attracts the dislocation in the tangential direction when the dislocation is close to the inclusion.

7. Conclusions

The interaction problem of a dislocation and collinear rigid lines embedded in a piezoelectric media is addressed. The lines considered are for either conductors or dielectrics. We obtain a closed form solution using the complex potential method, and explicitly derive field intensity factors and the forces on the dislocation for a single inclusion case.We present numerical examples and discuss the results.

References

[Chen et al. 2002] B. J. Chen, Z. M. Xiao, and L. K. M., "On the interaction between a semi-infinite anti-crack and a screw dislocation in piezoelectric solid", *Int. J. Solids Struct.* **39**:6 (2002), 1505–1513.

[Deng and Meguid 1998] W. Deng and S. A. Meguid, "Analysis of conducting rigid inclusions at the interface of two dissimilar piezoelectric materials", *J. Appl. Mech.* (*ASME*) **65** (1998), 76–84.

[Deng and Meguid 1999] W. Deng and S. A. Meguid, "Analysis of a screw dislocation inside an elliptical inhomogeneity in piezoelectric solids", *Int. J. Solids Struct.* **36**:10 (1999), 1449–1469.

[Fan and Keer 1993] H. Fan and L. M. Keer, "Two-dimensional line defects in anisotropic elastic solids", *Int. J. Fract.* **62**:1 (1993), 25–42.

[Gao and Fan 2000] C. F. Gao and W. X. Fan, "The generalized 2D problem of piezoelectric media with collinear rigid line inclusions", *Chin. J. Appl. Mech.* **17** (2000), 126–130.

[Huang and Kuang 2001] Z. Huang and Z. B. Kuang, "Dislocation inside a piezoelectric media with an elliptical inhomogeneity", *Int. J. Solids Struct.* **38**:46–47 (2001), 8459–8479.

[Kattis et al. 1998] M. A. Kattis, E. Providas, and A. L. Kalamkarov, "Two-phone potentials in the analysis of smart composites having piezoelectric components", *Compos. B Eng.* **29**:1 (1998), 9–14.

[Liang et al. 1995] J. Liang, J. C. Han, and S. Y. Du, "Rigid line inclusions and cracks in anisotropic piezoelectric solids", *Mech. Res. Commun.* **22**:1 (1995), 43–49.

[Liu and Fang 2003] Y. W. Liu and Q. H. Fang, "Electro-elastic interaction between a piezoelectric screw dislocation and circular interfacial rigid lines", *Int. J. Solids Struct.* **40**:20 (2003), 5353–5370.

[Meguid and Zhong 1997] S. A. Meguid and Z. Zhong, "Electroelastic analysis of a piezoelectric elliptical inhomogeneity", *Int. J. Solids Struct.* **34**:26 (1997), 3401–3414.

[Muskhelishvili 1975] N. I. Muskhelishvili, *Some basic problems of the mathematical theory of elasticity*, Noordhoff, Leiden, 1975.

[Pak 1990] Y. E. Pak, "Force on a piezoelectric screw dislocation", *J. Appl. Mech.* (*ASME*) **57** (1990), 863–869.

[Pak 1992a] Y. E. Pak, "Circular inclusion problem in anti-plane piezoelectricity", *Int. J. Solids Struct.* **29**:19 (1992), 2403–2419.

[Pak 1992b] Y. E. Pak, "Linear electro-elastic fracture mechanics of piezoelectric materials", *Int. J. Fract.* **54**:1 (1992), 79–100.

[Shi 1997] W. Shi, "Rigid line inclusions under anti-plane deformation and in-plane electric field in piezoelectric materials", *Eng. Fract. Mech.* **56**:2 (1997), 265–274.

Received 8 Dec 2005. Revised 9 Feb 2006. Accepted 16 Jul 2006.

BINGJIN CHEN: mbjchen@ntu.edu.sg
School of Mechanical and Aerospace Engineering, Nanyang Technological University, Nanyang Avenue, Singapore 639798

DONGWEI SHU: mdshu@ntu.edu.sg
School of Mechanical and Aerospace Engineering, Nanyang Technological University, Nanyang Avenue, Singapore 639798

ZHONGMIN XIAO: mzxiao@ntu.edu.sg
School of Mechanical and Aerospace Engineering, Nanyang Technological University, Nanyang Avenue, Singapore 639798